

1 **More Severe Hydrological Drought Events Emerge at Different Warming Levels**
2 **over the Wudinghe Watershed in northern China**

3 Yang Jiao^{1,2}, Xing Yuan^{1,2*}

4 ¹School of Hydrology and Water Resources, Nanjing University of Information
5 Science and Technology, Nanjing, 210044, Jiangsu, China

6 ²Key Laboratory of Regional Climate-Environment for Temperate East Asia
7 (RCE-TEA), Institute of Atmospheric Physics, Chinese Academy of Sciences, Beijing,
8 100029, China

9
10 *Hydrology and Earth System Sciences*

11 Submitted May 8, 2018

12 Revised September 29, 2018

13

*Corresponding author address: Xing Yuan, School of Hydrology and Water Resources, Nanjing University of Information Science and Technology, Nanjing, 210044, Jiangsu, China. E-mail: yuanxing@tea.ac.cn

14 **Abstract**

15 Assessment of changes in hydrological droughts at specific warming levels is
16 important for an adaptive water resources management with consideration of the 2015
17 Paris Agreement. However, most studies focused on the response of drought
18 frequency to the warming and neglected other drought characteristics including
19 severity. By using a semiarid watershed in northern China (i.e., Wudinghe) as an
20 example, here we show less frequent but more severe hydrological drought events
21 emerge at 1.5, 2 and 3 °C warming levels. We used meteorological forcings from eight
22 Coupled Model Intercomparison Project Phase 5 climate models under four
23 representative concentration pathways, to drive a newly developed land surface
24 hydrological model to simulate streamflow, and analyzed historical and future
25 hydrological drought characteristics based on the Standardized Streamflow Index. The
26 Wudinghe watershed will reach the 1.5/2/3 °C warming level around
27 2015-2034/2032-2051/2060-2079, with an increase of precipitation by 8%/9%/18%
28 and runoff by 27%/19%/44%, and a drop of hydrological drought frequency by
29 11%/26%/23% as compared to the baseline period (1986-2005). However, the drought
30 severity will rise dramatically by 184%/116%/184%, which is mainly caused by the
31 increased variability of precipitation and evapotranspiration. The climate models and
32 the land surface hydrological model contribute to more than 80% of total uncertainties
33 in the future projection of precipitation and hydrological droughts. This study
34 suggests that different aspects of hydrological droughts should be carefully
35 investigated when assessing the impact of 1.5, 2 and 3 °C global warming.

36

37 **Key Words:** hydrological drought; 1.5, 2 and 3 °C warming levels; CMIP5 models;

38 RCP scenarios; uncertainty analysis.

39

40 **1. Introduction**

41 Global warming has affected both natural and artificial systems across continents,
42 bringing a lot of eco-hydrological crises to many countries (Gitay et al., 2002; Tirado
43 et al., 2010; Thornton et al., 2014). The Intergovernmental Panel on Climate Change
44 (IPCC) Fifth Assessment Report (AR5) concluded that global average surface air
45 temperature increased by 0.61°C in 1986-2005 compared to pre-industrial periods
46 (IPCC, 2014a). In order to mitigate global warming, the Conference of the Parties of
47 the United Nations Framework Convention on Climate Change (UNFCCC)
48 emphasized in the Paris Agreement that the increase in global average temperature
49 should be controlled within 2 °C above preindustrial levels, and further efforts should
50 be made to limit it below 1.5 °C. However, whether the temperature controlling goal
51 can be reached is still unknown, with much difficulty under current emission
52 conditions (Peters et al., 2012). In addition, specific warming level such as 2 °C
53 increase would be too high for many regions and countries (James et al., 2017; Rogelj
54 et al., 2015). Therefore, it is necessary to assess changes in regional hydrological
55 cycle and extremes under 1.5, 2 and even 3 °C global warming.

56 Global warming is mainly caused by greenhouse gases emissions and has a profound
57 influence on hydrosphere and ecosphere (Barnett et al., 2005; Vorosmarty et al., 2000).
58 It alters hydrological cycle both directly (e.g., influences precipitation and
59 evapotranspiration) and indirectly (e.g., influences plant growth and related
60 hydrological processes) at global (Zhu et al., 2016; McVicar et al., 2012) and local
61 scales (Tang et al., 2013; Zheng et al., 2009; Zhang et al., 2008). Besides affecting the

62 mean states of the hydrological conditions, global warming also intensifies
63 hydrological extremes significantly, such as droughts which were regarded as
64 naturally occurring events when water (precipitation, or streamflow, etc.) is
65 significantly below normal over a period of time (Van Loon et al., 2016; Dai, 2011).
66 Among different types of droughts, hydrological droughts focus on the decrease in the
67 availability of water resources, e.g., surface and/or ground water (Lorenzo-Lacruz et
68 al., 2013). Many researchers paid attention to the historical changes, future evolutions
69 and uncertainties, and causing factors for hydrological droughts (Chang et al., 2016;
70 Kormos et al., 2016; Orlowsky and Seneviratne, 2013; Parajka et al., 2016; Perez et
71 al., 2011; Prudhomme et al., 2014; Van Loon and Laaha, 2015; Wanders and Wada,
72 2015; Yuan et al., 2017). Most drought projection studies focused on the future
73 changes over a fixed time period (e.g., late 21st century), but recent studies pointed out
74 the importance on hydrological drought evolution at certain warming levels (Roudier
75 et al., 2016; Marx et al., 2018) given the aim of the Paris Agreement. Moreover, the
76 changes in characteristics (e.g., frequency, duration, severity) of hydrological drought
77 events at specific warming levels received less attention. The projection of these
78 drought characteristics could provide more relevant guidelines for policymakers on
79 implementing adaptation strategies.

80 In the past five decades, a significant decrease in channel discharge was observed in
81 the middle reaches of the Yellow River basin over northern China (Yuan et al., 2018;
82 Zhao et al., 2014), leading to an intensified water resources scarcity in this populated
83 area. In this study, we take a semiarid watershed, the Wudinghe in the middle reaches

84 of the Yellow River basin as a testbed, aiming at solving the following questions: (1)
85 How do hydrological drought characteristics change at different warming levels over
86 the Wudinghe watershed? (2) What are the causes for the hydrological drought change?
87 (3) What are the contributions of uncertainties from different sources (e.g., climate
88 and land surface hydrological models, representative concentration pathways (RCPs)
89 scenarios, and internal variability)?

90 **2. Study area and dataset**

91 In this study, the Wudinghe watershed was chosen for hydrological drought analysis.
92 As one of the largest sub-basins of the Yellow River basin, the Wudinghe watershed is
93 located in the Loess Plateau, and has a drainage area of 30261 km² with Baijiachuan
94 hydrological station as the watershed outlet (Figure 1). It has a semiarid climate with
95 long-term (1956-2010) annual mean precipitation of 356 mm and runoff of 39 mm,
96 resulting in a runoff coefficient of 0.11 (Jiao et al., 2017). Most of the rainfall events
97 are concentrated in summer (June to September) with a large possibility of heavy
98 rains (Mo et al., 2009). Located in the transition zone between cropland/grassland and
99 desert/shrub, the northwest part of the Wudinghe watershed is dominated by sandy
100 soil, while the major soil type for the southeast part is loess soil. During recent
101 decades, the Wudinghe watershed has experienced a significant streamflow decrease
102 (Yuan et al., 2018; Zhao et al., 2014) and suffered from serious water resource
103 scarcity because of climate change, vegetation degradation and human water
104 consumption (Xiao, 2014; Xu, 2011).

105 <Figure 1 here>

106 The Coupled Model Intercomparison Project Phase 5 (CMIP5) general circulation
107 model (GCM) simulations for historical experiments and future projections formed
108 the science basis for the IPCC AR5 reports (IPCC, 2014b; Taylor et al., 2012). In this
109 study, we chose eight CMIP5 GCMs for historical (1961-2005) and future (2006-2099)
110 drought analysis, as they provided daily simulations under all four RCP scenarios (i.e.
111 RCP2.6/4.5/6.0/8.5). Table 1 listed the details of GCMs used in this paper. Because of
112 the deficiency in GCM precipitation and runoff simulations, we used the corrected
113 meteorological forcing data from CMIP5 climate models, to drive a high resolution
114 land surface hydrological model to simulate runoff and streamflow (see Section 3.1
115 for details).

116 <Table 1 here>

117 All CMIP5 simulations were bias corrected before being used as land surface model
118 input. After interpolating CMIP5 simulations and China Meteorological
119 Administration (CMA) station observations to the same resolution (0.01 degree in this
120 study), a modified correction method (Li et al., 2010) based on widely-used quantile
121 mapping (Wood et al., 2002; Yuan et al., 2015) was applied to adjust CMIP5/ALL
122 historical simulations and CMIP5/RCPs future simulations for each model at each
123 grid cell separately. The bias-corrected daily precipitation and temperature were then
124 further temporally disaggregated to a 6-hours interval based on the diurnal cycle
125 information from CRUNCEP 6-hourly dataset
126 (<https://svn-ccsm-inputdata.cgd.ucar.edu/trunk/inputdata/atm/datm7/>). Other 6-hourly
127 meteorological forcings, i.e., incident solar radiation, air pressure, specific humidity

128 and wind speed, were directly taken from CRUNCEP data.

129 **3. Land Surface Hydrological Model and Methods**

130 **3.1. Introduction of the CLM-GBHM model**

131 In this study, we chose a newly developed land surface hydrological model,
132 CLM-GBHM, to simulate historical and future streamflow. This model was first
133 developed and applied in the Wudinghe watershed at 0.01 degree (Jiao et al., 2017)
134 and then the Yellow River basin at 0.05 degree resolution (Sheng et al., 2017). By
135 improving surface runoff generation, subsurface runoff scheme, river network-based
136 representation and 1-D kinematic wave river routing processes, CLM-GBHM showed
137 good performances in simulating streamflow, soil moisture content and water table
138 depth (Sheng et al., 2017). Figure 2 demonstrated the structure and main
139 eco-hydrological processes of CLM-GBHM. Model resolution, surface datasets,
140 initial conditions and model parameters were kept consistent with Jiao et al. (2017),
141 except that monthly LAI in 1982 was used for all simulations because of an unknown
142 vegetation condition in the future.

143 <Figure 2 here>

144 **3.2. Determination of years reaching specific warming levels**

145 IPCC AR5 (IPCC, 2014a) reported that global average surface air temperature change
146 between pre-industrial period (1850-1900) and reference period (1986-2005) is 0.61
147 (0.55 to 0.67) °C. Therefore, we took 1986-2005 as the baseline period. Monthly
148 standardized streamflow index (SSI) simulations from CLM-GBHM were compared
149 with the observed records during the baseline period, and the model performed well

150 with a correlative coefficient of 0.53 ($p < 0.01$). Here, “1.5 °C warming level” referred
151 to a global temperature increase of 0.89 ($= 1.5 - 0.61$) °C, “2 °C warming level” referred
152 to an increase of 1.39 ($= 2 - 0.61$) °C, and “3 °C warming level” referred to an increase
153 of 2.39 ($= 3 - 0.61$) °C compared with the baseline, respectively. As large differences
154 existed in temperature simulations among CMIP5 models and RCP scenarios, we
155 applied a widely used time sampling method (James et al., 2017; Mohammed et al.,
156 2017; Marx et al., 2018) to each GCM under each RCP scenario (referred to as
157 GCM/RCP combination hereafter). A 20-years moving window, which has the same
158 length of the baseline period, was used to determine the first period reaching a
159 specific warming level for each combination, with the period median year referred to
160 as the “crossing year”.

161 **3.3. Identification of hydrological drought characteristics**

162 We used a two-step method similar to previous studies (Lorenzo-Lacruz et al., 2013;
163 Ma et al., 2015; Yuan et al., 2017) to extract hydrological drought characteristics in
164 this paper. At the first step, a hydrological drought index named as Standardized
165 Streamflow Index (SSI) was calculated by fitting monthly streamflow using a
166 probabilistic distribution function (Vicente-Serrano et al., 2012; Yuan et al., 2017).
167 Specifically, for each calendar month, streamflow values in that month during
168 baseline period were collected, arranged, and fitted by using a gamma distribution
169 function. Using the same parameters of the fitted gamma distribution, both baseline
170 (1986-2005) and future (2006-2099) streamflow values in that calendar month were
171 standardized to get SSI values. The procedure was repeated for twelve calendar

172 months, four RCP scenarios and eight GCMs separately. The second step was
173 identification and characterization of hydrological drought events by an SSI threshold
174 method (Yuan and Wood, 2013; Lorenzo-Lacruz et al., 2013; Van Loon and Laaha,
175 2015). Here, a threshold of -0.8 was selected, which is equivalent to a dry condition
176 with a probability of 20%. Months with SSI below -0.8 were treated as dry months,
177 and 3 or more continuous dry months were considered as the emergence of a
178 hydrological drought event. To characterize the hydrological drought event, drought
179 duration (months) and severity (sum of the difference between -0.8 and SSI) for a
180 certain drought event were calculated. As future SSI values were all calculated based
181 on historical values, it is important to mention that drought analysis here represented
182 those without adaptation (Samaniego et al., 2018).

183 **3.4. Uncertainty separation**

184 Given large spreads among future projections (including combinations of eight GCMs
185 and four RCP scenarios, as shown in shaded areas in Figure 3), a separation method
186 (Hawkins and Sutton, 2009; Orłowsky and Seneviratne, 2013) was applied to explore
187 uncertainty from three individual sources, i.e., internal variability, climate models and
188 RCPs scenarios. In order to separate internal variability from other two factors with
189 long-term trends, a 4th order polynomial was selected to fit specific time series: the
190 fitting was first carried out during baseline period (1986-2005) to obtain an average i_m
191 as a reference value, and then during future period (2006-2099) to obtain a smooth fit
192 $x_{m,s,t}$. Future projections ($X_{m,s,t}$) were then separated into three parts: reference value
193 (i_m), smooth fit ($x_{m,s,t}$) and residual ($e_{m,s,t}$), and the uncertainties from three sources

194 were then calculated as follows:

$$V = \sum_m \text{var}_{s,t}(e_{m,s,t}) / N_m \quad (1)$$

$$M_t = \sum_s \text{var}_m(x_{m,s,t}) / N_s \quad (2)$$

$$S_t = \text{var}_s(\sum_m x_{m,s,t} / N_m) \quad (3)$$

195 where V , M_t and S_t represent uncertainties from internal variability (which is
196 time-invariant), climate models and RCPs scenarios, N_m and N_s are numbers of
197 climate models and RCPs scenarios, $\text{var}_{s,t}$ denotes the variance across scenarios and
198 time, var_m and var_s are variances across models and scenarios respectively. Finally,
199 uncertainty contributions from each component were calculated as proportions to the
200 sum. In this study, we applied this method to the 20-years moving averaged ensemble
201 time series.

202 **4. Results**

203 **4.1. Changes in hydrometeorology in the past and future**

204 We first calculated the trends during both the historical and future periods for
205 basin-averaged annual mean hydrological variables (Table 2 and Figure 3). During
206 1961-2005, there was a significant increasing trend ($p < 0.01$) in observed temperature
207 and a decreasing trend ($p < 0.1$) in observed precipitation, resulted in a decreasing
208 naturalized streamflow ($p < 0.01$) and an increasing hydrological drought frequency
209 ($p < 0.01$). Here, the naturalized streamflow was obtained by adding human water use
210 back to the observed streamflow (Yuan et al., 2017). These historical changes could
211 be captured by hydro-climate model simulations to some extent, although both the
212 warming and drying trends were underestimated (Table 2). Ensemble monthly SSI

213 series from GCM driven model simulations were also compared with offline results
214 (CRUNCEP driven) during historical period, resulted in a correlative coefficient of
215 0.47 ($p < 0.01$). During 2006-2099, four variables show consistent changing trends
216 across RCPs scenarios, but with different magnitudes (Table 2). Future temperature
217 and precipitation will increase, resulting in an increasing streamflow and decreasing
218 hydrological drought frequency. Unlike temperature trends that increase from RCP2.6
219 to RCP8.5 (which indicates different radiative forcings), precipitation trend under
220 RCP6.0 is smaller than that under RCP4.5, suggesting a nonlinear response of
221 regional water cycle to the increase in radiative forcings. As a result, RCP6.0 shows
222 the smallest increasing rate in streamflow and decreasing rate in drought frequency.

223 <Table 2 here>

224 More details could be found in Figure 3 when focusing on dynamic changes in the
225 history and future. Figure 3a shows that the differences in temperature among RCPs
226 are negligible until 2030s when RCP8.5 starts to outclass other scenarios, and the
227 others begin to diverge in the far future (2060s-2080s). In contrast, differences in
228 future precipitation are small throughout the 21st century, except that RCP8.5 scenario
229 becomes larger after 2080s (Figure 3b). As comprehensive outcomes of climate and
230 eco-hydrological factors, a clear decrease-increase pattern in streamflow and an
231 increase-decrease trend in hydrological drought frequency are found (Figure 3c and
232 3d). However, differences among RCPs are not discernible. Figures 3b-3d also show
233 that the differences in water-related variables among climate models are very large.

234 <Figure 3 here>

235 Using the time-sampling method mentioned in Section 3.2, first 20-year periods with
236 mean temperature increasing across 1.5, 2 and 3 °C warming levels for each
237 GCM/RCP combination were identified and listed in Table 3. To demonstrate the
238 overall situation for a specific warming level, we chose median year among GCMs as
239 model ensemble for each RCP scenario, and median year among all GCMs and RCPs
240 as total ensemble. GCM/RCP combinations not reaching specific warming level were
241 marked as “NR” in Table 3 and were not considered when calculating ensemble year.

242 <Table 3 here>

243 As listed in Table 3, crossing years for most GCM/RCP combinations reaching 1.5 °C
244 warming level are before 2032 except for GFDL-ESM2M and MRI-CGCM3. Model
245 ensemble years for different RCP scenarios have small differences, and total ensemble
246 year for all GCMs and RCPs is 2025, indicating that 1.5 °C warming level would be
247 reached within 2015-2034. As for 2 and 3 °C warming level, the total ensemble year is
248 2042 and 2070, respectively. There are large differences in crossing years among
249 different GCMs, ranging from 2016 to 2075 for 1.5 °C, 2030 to 2076 for 2 °C, and
250 2051 to 2086 for 3 °C. Generally, three global warming thresholds would be reached
251 first under RCP8.5 and last under RCP6.0 scenario. All GCMs will not reach 3 °C
252 warming level under RCP2.6, while under other RCP scenarios this temperature
253 increase would probably be reached around 2073 or even as early as 2050s.

254 **4.2. Hydrological changes at 1.5, 2 and 3 °C warming levels**

255 After identifying the time periods reaching specific warming levels, we collected
256 precipitation and runoff data within these periods (different among GCM/RCP

257 combinations), and calculated their relative changes compared to the baseline period
258 (1986-2005). Figure 4 shows the spatial pattern of relative changes in model ensemble
259 mean precipitation of these time periods, except for the period under RCP2.6 at 3 °C
260 warming level during which no sample exists. Results indicate that precipitation will
261 increase at all warming levels and all RCP scenarios, while differences exist in spatial
262 patterns. The ensemble mean precipitation increases by 8.0%, 9.1% and 18.0% at 1.5,
263 2 and 3 °C warming levels for all RCP scenarios respectively, indicating larger
264 increase in precipitation when warming level increases. For each warming level,
265 precipitation changes among all RCP scenarios are quite close except for RCP6.0 at
266 3 °C warming level. Larger precipitation increases generally occur in the south and
267 southwest parts which are upstream regions of the Wudinghe watershed.

268 <Figure 4 here>

269 The watershed-mean runoff increases by 26.7%, 18.7% and 44.5% at each warming
270 level respectively, which are larger than those of precipitation because of nonlinear
271 hydrological response (Figure 5). For all warming levels, RCP8.5 shows greatest
272 runoff increase and RCP2.6/6.0 the lowest. Small or negative changes in runoff
273 emerge in the north and southeast regions under RCP2.6/4.5/6.0 scenarios (Figure 5),
274 where precipitation increases the least (Figure 4). Besides, runoff changes are also
275 closely linked to watershed river networks, with large increase in the south and
276 middle parts (upper and middle reaches) and small increase or even decrease in the
277 southeast and northeast parts (lower reaches), showing the redistribution effect of
278 surface topography and soil property.

279 <Figure 5 here>

280 Figure 6 shows the characteristics of hydrological droughts during baseline period and
281 the periods reaching all warming levels. The number of hydrological drought events
282 averaged among all RCP scenarios and climate models is 7 in the baseline period, and
283 it drops to 6.2 (-11% relative to baseline, the same below) at 1.5 °C, 5.2 (-26%) at
284 2 °C and 5.4 (-23%) at 3 °C warming levels (Figure 6a). However, hydrological
285 drought duration increases from 5 months at baseline to 6.5 (+30%), 5.9 (+18%) and 6
286 months (+20%) at 1.5, 2 and 3 °C warming levels, respectively. Drought severity
287 increases dramatically from 1.9 at baseline to 5.4 (+184%) at 1.5 °C warming level,
288 and then drops to 4.1 (+116%) at 2 °C warming level and rebounds to 5.4 (+184%) at
289 3 °C warming level (Figure 6a). These results indicate that although precipitation and
290 runoff increase, the Wudinghe watershed would suffer from more severe hydrological
291 events in the near future at 1.5 °C warming level. The severity could be alleviated in
292 time periods reaching 2 °C warming level, with more precipitation occurring over the
293 watershed.

294 <Figure 6 here>

295 The analysis on individual scenarios suggests a similar conclusion (Figures 6b-6e).
296 Drought amount and severity increase generally when radiative forcing increases. The
297 least changes in drought severity are found under RCP4.5 scenario while the largest
298 changes are under RCP6.0 scenario. Higher warming levels could lead to more
299 moderate drought events under low emission scenarios (RCP2.6/4.5) because of more
300 precipitation in the near future, while high emissions (RCP6.0/8.5) would increase the

301 risk of hydrological drought significantly.

302 **5. Discussion**

303 To explore the reason for less frequent but more severe hydrological droughts, we
304 compared the differences in monthly precipitation, evapotranspiration,
305 total/surface/sub-surface runoff and streamflow between the baseline period and
306 periods reaching 1.5, 2 and 3 °C warming levels. Standardized indices for these
307 hydrological variables were used to remove seasonality from monthly time series, and
308 mean values and variabilities of these indices were chosen as indicators.

309 <Figure 7 here>

310 Figure 7 shows that mean values increase as temperature increases for all standardized
311 hydrological indices, showing a wetter hydroclimate in the future with more
312 precipitation, evapotranspiration, runoff and streamflow (Figure 7a). However,
313 variabilities for the standardized indices in the future are much higher than those
314 during baseline period, indicating larger fluctuations and higher chance for extreme
315 droughts/floods at all warming levels (Figure 7b). For extreme drought events (with
316 an SSI < -1.3, representing a dry condition with a probability of 10%), the ensemble
317 mean amount of drought events are 4.3, 3.1 and 3.7 at 1.5, 2 and 3 °C warming levels,
318 which are much larger than the baseline period with 0.9 (not shown). Focusing on the
319 gaps between baseline and future periods, it is clear that the differences in both
320 evapotranspiration and runoff are larger than those of precipitation for mean values
321 and standard deviations, suggesting the water redistribution through complicated
322 hydrological processes. The increase in mean value of runoff and consequently

323 streamflow mainly comes from the increase in subsurface runoff. As hydrological
324 drought defined in this paper is based on monthly SSI series, increases in both mean
325 value and variability in precipitation and evapotranspiration indicate a period with
326 less frequent but more severe hydrological drought events.

327 Another issue is the reliability of results considering large differences among CMIP5
328 models. Figure 8 shows the uncertainty fractions contributed from internal variability,
329 climate models and RCPs scenarios based on multi-model and multi-scenario
330 ensemble projections of temperature, precipitation, streamflow and drought frequency.
331 Uncertainty in temperature projection is mainly contributed by climate models before
332 2052, and it is then taken over by RCPs scenarios. Internal variability contributes to
333 less than 1.5% of the uncertainty for the temperature projection (Figure 8a). For
334 precipitation projection, climate models account for a large proportion of uncertainty
335 throughout the century. The internal variability contributes to larger uncertainty than
336 RCPs scenarios until the second half of the 21st century (Figure 8b). Similar to
337 precipitation, major source of uncertainty for the projections of streamflow and
338 hydrological drought frequency comes from climate and land surface hydrological
339 models, while the impacts of both internal variability and RCP scenarios are further
340 weakened (Figures 8c-8d).

341 <Figure 8 here>

342 Model accounts for over 80% of total uncertainties, while internal variability
343 contributes to a comparable or larger proportion than RCPs scenarios, for all variables
344 except temperature (see Table 4). RCPs scenario uncertainty accounts for 14.3% of

345 temperature uncertainty at 1.5 °C warming level with this proportion increasing to
346 33% (63.7%) at 2 °C (3 °C) warming level, while its contribution to precipitation
347 uncertainty remains less than 10%. RCPs scenario only contributes to around 5% of
348 the uncertainties in the projections of streamflow and hydrological drought frequency.
349 These results indicate that the improvement in GCM simulated precipitation would
350 largely narrow the uncertainties for future projections of hydrological droughts.
351 Besides, previous studies (Marx et al., 2018; Samaniego et al., 2018) have shown that
352 uncertainties contributed from land surface hydrological models can be comparable to
353 that from GCMs, indicating the importance of introducing multiple land surface
354 hydrological models into the analysis of uncertainty, and the significance of exploring
355 more suitable methods in further studies.

356 <Table 4 here>

357 There are also some issues for further investigations. As shown in Figure 3, GCM
358 historical simulations underestimates the increasing trend in temperature and
359 decreasing trend in precipitation, and results in underestimations of hydrological
360 drying trends. Although the quantile mapping method used in this study is able to
361 remove the biases in GCM simulations (e.g., mean value, variance), the
362 underestimation of trends could not be corrected. An alternative method is to use
363 regional climate models for dynamical downscaling, which would be useful if
364 regional forcings (e.g., topography, land use change, aerosol emission) are strong.
365 Another issue is about the spatially varied warming rates. IPCC AR5 reported (IPCC,
366 2014c) that global warming for the last 20 years compared to pre-industrial are

367 0.3-1.7 °C (RCP2.6), 1.1-2.6 °C (RCP4.5), 1.4-3.1 °C (RCP6.0), 2.6-4.8 °C (RCP8.5).
368 However, temperature increases vary a lot for different regions. For instance,
369 temperature rises faster in high-altitude (Kraaijenbrink et al., 2017) and polar regions
370 (Bromwich et al., 2013), where the rate of regional warming could be three times of
371 global warming. Actually, reaching periods for regional warming thresholds in the
372 Wudinghe watershed are earlier than the global ones (not shown here), which suggest
373 that the regional warming would be more severe at specific global warming levels.

374 **6. Conclusions**

375 In this paper, we bias-corrected future projections of meteorological forcings from
376 eight CMIP5 GCM simulations under four RCP scenarios to drive a newly developed
377 land surface hydrological model, CLM-GBHM, to project changes in streamflow and
378 hydrological drought characteristics over the Wudinghe watershed. After determining
379 the time periods reaching 1.5, 2 and 3 °C global warming levels for each GCM/RCP
380 combination, we focused on the changes in regional hydrological drought
381 characteristics at all warming levels. Moreover, projection uncertainties from different
382 sources were separated and analyzed. Main conclusions are listed as follows:

383 (1) With CMIP5 GCM simulations as forcing data, the model ensemble mean hindcast
384 can reproduce the significant decreasing trend of streamflow and increasing trend of
385 hydrological drought frequency in historical period (1961-2005), but the drying trend
386 is underestimated because of GCM uncertainties. Streamflow increases and
387 hydrological drought frequency decreases in the future under all RCP scenarios.

388 (2) The time periods reaching 1.5, 2 and 3 °C warming levels over the Wudinghe

389 watershed are 2015-2034, 2032-2051 and 2060-2079, respectively. There are large
390 differences in results among different GCMs, while different RCP scenarios show
391 consistence in reaching periods with RCP8.5 the earliest and RCP6.0 the latest.

392 (3) Precipitation increases under all RCP scenarios at all warming levels (8%, 9% and
393 18%), while differences exist in spatial patterns. Runoff has larger relative change
394 rates (27%, 19% and 44%), with larger increases of runoff occurred in the upper and
395 middle reaches and less increases or even decreases emerged in the lower reaches,
396 indicating a complex spatial distribution in hydrological droughts.

397 (4) As a result of increasing mean values and variability for precipitation,
398 evapotranspiration and runoff, hydrological drought frequency drops by 11%-26% at
399 all warming levels compared to the baseline period, while hydrological drought
400 severity rises dramatically by 116%-184%. This indicates that the Wudinghe
401 watershed would suffer more severe hydrological drought events in the future,
402 especially under RCP6.0 and RCP8.5 scenarios.

403 (5) The main uncertainty sources vary among hydrological variables. Most
404 uncertainties are from climate and land surface models, especially for precipitation. At
405 all warming levels, models contribute to over 80% of total uncertainties, while
406 internal variability contributes to a comparable proportion of uncertainties to RCPs
407 scenarios for precipitation, streamflow and hydrological drought frequency.

408

409 **Acknowledgements**

410 We would like to thank the editor and two anonymous reviewers for their helpful

411 comments. This research was supported by National Key R&D Program of China
412 (2018YFA0606002), National Natural Science Foundation of China (91547103), and
413 the Startup Foundation for Introducing Talent of NUIST. Daily precipitation and
414 temperature simulated by CMIP5 models were provided by the World Climate
415 Research Programme's Working Group on Coupled Modeling
416 (<https://esgf-data.dkrz.de/search/cmip5-dkrz>). We thank Prof. Dawen Yang and Prof.
417 Huimin Lei for the implementation of the CLM-GBHM land surface hydrological
418 model.

419

420 **References**

- 421 Barnett, T. P., Adam, J. C., and Lettenmaier, D. P.: Potential impacts of a warming
422 climate on water availability in snow-dominated regions, *Nature*, 438, 303-309,
423 doi:10.1038/nature04141, 2005.
- 424 Bromwich, D. H., Nicolas, J. P., Monaghan, A. J., Lazzara, M. A., Keller, L. M.,
425 Weidner, G. A., and Wilson, A. B.: Central West Antarctica among the most
426 rapidly warming regions on Earth, *Nat Geosci*, 6, 139-145,
427 doi:10.1038/Ngeo1671, 2013.
- 428 Chang, J., Li, Y., Wang, Y., and Yuan, M.: Copula-based drought risk assessment
429 combined with an integrated index in the Wei River Basin, China, *Journal of*
430 *Hydrology*, 540, 824-834, doi:10.1016/j.jhydrol.2016.06.064, 2016.
- 431 Dai, A. G.: Drought under global warming: a review, *Wires Clim Change*, 2, 45-65,
432 doi:10.1002/wcc.81, 2011.
- 433 Gitay, H., Suárez, A., Watson, R. T., and Dokken, D. J.: Climate change and
434 biodiversity, IPCC Technical Paper V, 2002.
- 435 Hawkins, E., and Sutton, R.: The Potential to Narrow Uncertainty in Regional
436 Climate Predictions, *B Am Meteorol Soc*, 90, 1095-+,
437 doi:10.1175/2009bams2607.1, 2009.
- 438 IPCC: Climate Change 2013 - The Physical Science Basis, Cambridge University
439 Press, Cambridge, United Kingdom and New York, NY, USA, 1535 pp., 2014a.
- 440 IPCC: Summary for Policymakers, in: Climate Change 2013 - The Physical Science
441 Basis, edited by: Stocker, T. F., Qin, D., Plattner, G.-K., Tignor, M., Allen, S. K.,
442 Boschung, J., Nauels, A., Xia, Y., Bex, V., and Midgley, P. M., Cambridge
443 University Press, Cambridge, United Kingdom and New York, NY, USA, 1-30,
444 2014b.
- 445 IPCC: Long-term Climate Change: Projections, Commitments and Irreversibility, in:
446 Climate Change 2013 - The Physical Science Basis, edited by: Stocker, T. F.,
447 Qin, D., Plattner, G.-K., Tignor, M., Allen, S. K., Boschung, J., Nauels, A., Xia,
448 Y., Bex, V., and Midgley, P. M., Cambridge University Press, Cambridge,

449 United Kingdom and New York, NY, USA, 1029-1136, 2014c.

450 James, R., Washington, R., Schleussner, C. F., Rogelj, J., and Conway, D.:
451 Characterizing half-a-degree difference: a review of methods for identifying
452 regional climate responses to global warming targets, *Wires Clim Change*, 8,
453 doi:10.1002/wcc.457, 2017.

454 Jiao, Y., Lei, H. M., Yang, D. W., Huang, M. Y., Liu, D. F., and Yuan, X.: Impact of
455 vegetation dynamics on hydrological processes in a semi-arid basin by using a
456 land surface-hydrology coupled model, *Journal of Hydrology*, 551, 116-131,
457 doi:10.1016/j.jhydrol.2017.05.060, 2017.

458 Kormos, P. R., Luce, C. H., Wenger, S. J., and Berghuijs, W. R.: Trends and
459 sensitivities of low streamflow extremes to discharge timing and magnitude in
460 Pacific Northwest mountain streams, *Water Resour Res*, 52, 4990-5007,
461 doi:10.1002/2015wr018125, 2016.

462 Kraaijenbrink, P. D. A., Bierkens, M. F. P., Lutz, A. F., and Immerzeel, W. W.:
463 Impact of a global temperature rise of 1.5 degrees Celsius on Asia's glaciers,
464 *Nature*, 549, 257-+, doi:10.1038/nature23878, 2017.

465 Li, H. B., Sheffield, J., and Wood, E. F.: Bias correction of monthly precipitation and
466 temperature fields from Intergovernmental Panel on Climate Change AR4
467 models using equidistant quantile matching, *J Geophys Res-Atmos*, 115,
468 doi:10.1029/2009jd012882, 2010.

469 Lorenzo-Lacruz, J., Moran-Tejeda, E., Vicente-Serrano, S. M., and Lopez-Moreno, J.
470 I.: Streamflow droughts in the Iberian Peninsula between 1945 and 2005: spatial
471 and temporal patterns, *Hydrology and Earth System Sciences*, 17, 119-134,
472 doi:10.5194/hess-17-119-2013, 2013.

473 Ma, F., Yuan, X., and Ye, A. Z.: Seasonal drought predictability and forecast skill
474 over China, *J Geophys Res-Atmos*, 120, 8264-8275, doi:10.1002/2015jd023185,
475 2015.

476 Marx, A., Kumar, R., Thober, S., Rakovec, O., Wanders, N., Zink, M., Wood, E. F.,
477 Pan, M., Sheffield, J., and Samaniego, L.: Climate change alters low flows in
478 Europe under global warming of 1.5, 2, and 3 degrees C, *Hydrology and Earth*

479 System Sciences, 22, 1017-1032, doi:10.5194/hess-22-1017-2018, 2018.

480 McVicar, T. R., Roderick, M. L., Donohue, R. J., Li, L. T., Van Niel, T. G., Thomas,
481 A., Grieser, J., Jhajharia, D., Himri, Y., Mahowald, N. M., Mescherskaya, A. V.,
482 Kruger, A. C., Rehman, S., and Dinpashoh, Y.: Global review and synthesis of
483 trends in observed terrestrial near-surface wind speeds: Implications for
484 evaporation, Journal of Hydrology, 416, 182-205,
485 doi:10.1016/j.jhydrol.2011.10.024, 2012.

486 Mo, X. G., Liu, S. X., Chen, D., Lin, Z. H., Guo, R. P., and Wang, K.: Grid-size
487 effects on estimation of evapotranspiration and gross primary production over a
488 large Loess Plateau basin, China, Hydrolog Sci J, 54, 160-173,
489 doi:10.1623/hysj.54.1.160, 2009.

490 Mohammed, K., Islam, A. S., Islam, G. M. T., Alfieri, L., Bala, S. K., and Khan, M. J.
491 U.: Extreme flows and water availability of the Brahmaputra River under 1.5 and
492 2 A degrees C global warming scenarios, Climatic Change, 145, 159-175,
493 doi:10.1007/s10584-017-2073-2, 2017.

494 Orłowsky, B., and Seneviratne, S. I.: Elusive drought: uncertainty in observed trends
495 and short- and long-term CMIP5 projections, Hydrology and Earth System
496 Sciences, 17, 1765-1781, doi:10.5194/hess-17-1765-2013, 2013.

497 Parajka, J., Blaschke, A. P., Bloeschl, G., Haslinger, K., Hepp, G., Laaha, G.,
498 Schoener, W., Trautvetter, H., Viglione, A., and Zessner, M.: Uncertainty
499 contributions to low-flow projections in Austria, Hydrology and Earth System
500 Sciences, 20, 2085-2101, doi:10.5194/hess-20-2085-2016, 2016.

501 Perez, G. A. C., van Huijgevoort, M. H. J., Voss, F., and van Lanen, H. A. J.: On the
502 spatio-temporal analysis of hydrological droughts from global hydrological
503 models, Hydrology and Earth System Sciences, 15, 2963-2978,
504 doi:10.5194/hess-15-2963-2011, 2011.

505 Peters, G. P., Andrew, R. M., Boden, T., Canadell, J. G., Ciais, P., Le Quéré, C.,
506 Marland, G., Raupach, M. R., and Wilson, C.: The challenge to keep global
507 warming below 2 C, Nat Clim Change, 3, 4, 2012.

508 Prudhomme, C., Giuntoli, I., Robinson, E. L., Clark, D. B., Arnell, N. W., Dankers,

509 R., Fekete, B. M., Franssen, W., Gerten, D., Gosling, S. N., Hagemann, S.,
510 Hannah, D. M., Kim, H., Masaki, Y., Satoh, Y., Stacke, T., Wada, Y., and
511 Wisser, D.: Hydrological droughts in the 21st century, hotspots and uncertainties
512 from a global multimodel ensemble experiment, *Proceedings of the National*
513 *Academy of Sciences*, 111, 3262-3267, doi:10.1073/pnas.1222473110, 2014.

514 Rogelj, J., Luderer, G., Pietzcker, R. C., Kriegler, E., Schaeffer, M., Krey, V., and
515 Riahi, K.: Energy system transformations for limiting end-of-century warming to
516 below 1.5 degrees C, *Nat Clim Change*, 5, 519+, doi:10.1038/nclimate2572,
517 2015.

518 Roudier, P., Andersson, J. C. M., Donnelly, C., Feyen, L., Greuell, W., and Ludwig,
519 F.: Projections of future floods and hydrological droughts in Europe under a+2
520 degrees C global warming, *Climatic Change*, 135, 341-355,
521 doi:10.1007/s10584-015-1570-4, 2016.

522 Samaniego, L., Thober, S., Kumar, R., Wanders, N., Rakovec, O., Pan, M., Zink, M.,
523 Sheffield, J., Wood, E., and Marx, A.: Anthropogenic warming exacerbates
524 European soil moisture droughts, *Nat Clim Change*, 8, 421, 2018, doi:
525 10.1038/s41558-018-0138-5

526 Sheng, M. Y., Lei, H. M., Jiao, Y., and Yang, D. W.: Evaluation of the Runoff and
527 River Routing Schemes in the Community Land Model of the Yellow River
528 Basin, *J Adv Model Earth Sy*, 9, 2993-3018, doi:10.1002/2017ms001026, 2017.

529 Tang, Y., Tang, Q., Tian, F., Zhang, Z., and Liu, G.: Responses of natural runoff to
530 recent climatic variations in the Yellow River basin, China, *Hydrology and Earth*
531 *System Sciences*, 17, 4471-4480, doi: 10.5194/hess-17-4471-2013, 2013.

532 Taylor, K. E., Stouffer, R. J., and Meehl, G. A.: An Overview of Cmp5 and the
533 Experiment Design, *B Am Meteorol Soc*, 93, 485-498,
534 doi:10.1175/Bams-D-11-00094.1, 2012.

535 Thornton, P. K., Ericksen, P. J., Herrero, M., and Challinor, A. J.: Climate variability
536 and vulnerability to climate change: a review, *Global Change Biol*, 20,
537 3313-3328, doi:10.1111/gcb.12581, 2014.

538 Tirado, M. C., Clarke, R., Jaykus, L. A., McQuatters-Gollop, A., and Franke, J. M.:

539 Climate change and food safety: A review, *Food Res Int*, 43, 1745-1765,
540 doi:10.1016/j.foodres.2010.07.003, 2010.

541 Van Loon, A. F., and Laaha, G.: Hydrological drought severity explained by climate
542 and catchment characteristics, *Journal of Hydrology*, 526, 3-14,
543 doi:10.1016/j.jhydrol.2014.10.059, 2015.

544 Van Loon, A. F., Stahl, K., Di Baldassarre, G., Clark, J., Rangelcroft, S., Wanders, N.,
545 Gleeson, T., Van Dijk, A. I. J. M., Tallaksen, L. M., Hannaford, J., Uijlenhoet, R.,
546 Teuling, A. J., Hannah, D. M., Sheffield, J., Svoboda, M., Verbeiren, B.,
547 Wagener, T., and Van Lanen, H. A. J.: Drought in a human-modified world:
548 reframing drought definitions, understanding, and analysis approaches,
549 *Hydrology and Earth System Sciences*, 20, 3631-3650,
550 doi:10.5194/hess-20-3631-2016, 2016.

551 Vicente-Serrano, S. M., Lopez-Moreno, J. I., Begueria, S., Lorenzo-Lacruz, J.,
552 Azorin-Molina, C., and Moran-Tejeda, E.: Accurate Computation of a
553 Streamflow Drought Index, *J Hydrol Eng*, 17, 318-332,
554 doi:10.1061/(Asce)He.1943-5584.0000433, 2012.

555 Vorosmarty, C. J., Green, P., Salisbury, J., and Lammers, R. B.: Global water
556 resources: Vulnerability from climate change and population growth, *Science*,
557 289, 284-288, doi:10.1126/science.289.5477.284, 2000.

558 Wanders, N., and Wada, Y.: Human and climate impacts on the 21st century
559 hydrological drought, *Journal of Hydrology*, 526, 208-220,
560 doi:10.1016/j.jhydrol.2014.10.047, 2015.

561 Wood, A. W., Maurer, E. P., Kumar, A., and Lettenmaier, D. P.: Long-range
562 experimental hydrologic forecasting for the eastern United States, *J Geophys*
563 *Res-Atmos*, 107, doi:10.1029/2001jd000659, 2002.

564 Xiao, J. F.: Satellite evidence for significant biophysical consequences of the "Grain
565 for Green" Program on the Loess Plateau in China, *J Geophys Res-Biogeo*, 119,
566 2261-2275, doi:10.1002/2014jg002820, 2014.

567 Xu, J. X.: Variation in annual runoff of the Wudinghe River as influenced by climate
568 change and human activity, *Quatern Int*, 244, 230-237,

569 doi:10.1016/j.quaint.2010.09.014, 2011.

570 Yuan, X., and Wood, E. F.: Multimodel seasonal forecasting of global drought onset,
571 Geophys Res Lett, 40, 4900-4905, doi:10.1002/grl.50949, 2013.

572 Yuan, X., Roundy, J. K., Wood, E. F., and Sheffield, J.: Seasonal forecasting of
573 global hydrologic extremes: system development and evaluation over GEWEX
574 basins, B Am Meteorol Soc, 96, 1895-1912, doi:10.1175/BAMS-D-14-00003.1,
575 2015.

576 Yuan, X., Zhang, M., Wang, L. Y., and Zhou, T.: Understanding and seasonal
577 forecasting of hydrological drought in the Anthropocene, Hydrology and Earth
578 System Sciences, 21, 5477-5492, doi:10.5194/hess-21-5477-2017, 2017.

579 Yuan, X., Y. Jiao, D. Yang, and H. Lei: Reconciling the attribution of changes in
580 streamflow extremes from a hydroclimate perspective, Water Resour Res,
581 doi:10.1029/2018WR022714, 2018

582 Zhang, X. P., Zhang, L., Zhao, J., Rustomji, P., and Hairsine, P.: Responses of
583 streamflow to changes in climate and land use/cover in the Loess Plateau, China,
584 Water Resour Res, 44, doi:10.1029/2007wr006711, 2008.

585 Zhao, G. J., Tian, P., Mu, X. M., Jiao, J. Y., Wang, F., and Gao, P.: Quantifying the
586 impact of climate variability and human activities on streamflow in the middle
587 reaches of the Yellow River basin, China, Journal of Hydrology, 519, 387-398,
588 doi:10.1016/j.jhydrol.2014.07.014, 2014.

589 Zheng, H. X., Zhang, L., Zhu, R. R., Liu, C. M., Sato, Y., and Fukushima, Y.:
590 Responses of streamflow to climate and land surface change in the headwaters of
591 the Yellow River Basin, Water Resour Res, 45, doi:10.1029/2007wr006665,
592 2009.

593 Zhu, Z. C., Piao, S. L., Myneni, R. B., Huang, M. T., Zeng, Z. Z., Canadell, J. G.,
594 Ciais, P., Sitch, S., Friedlingstein, P., Arneeth, A., Cao, C. X., Cheng, L., Kato, E.,
595 Koven, C., Li, Y., Lian, X., Liu, Y. W., Liu, R. G., Mao, J. F., Pan, Y. Z., Peng,
596 S. S., Penuelas, J., Poulter, B., Pugh, T. A. M., Stocker, B. D., Viovy, N., Wang,
597 X. H., Wang, Y. P., Xiao, Z. Q., Yang, H., Zaehle, S., and Zeng, N.: Greening of
598 the Earth and its drivers, Nat Clim Change, 6, 791-795,

600 **Figure Captions**

601 **Figure 1.** Location, elevation and river networks for the Wudinghe watershed.

602 **Figure 2.** Structure and main eco-hydrological processes for the land surface
603 hydrological model CLM-GBHM. (modified from Jiao et al., 2017)

604 **Figure 3.** Historical (ALL) and future (RCP2.6/4.5/6.0/8.5) time series of
605 standardized annual mean (a) temperature, (b) precipitation and (c) streamflow, and (d)
606 the time series of hydrological drought frequency (drought months for each year) over
607 the Wudinghe watershed. Shaded areas indicate the ranges between maximum and
608 minimum values among CMIP5/CLM-GBHM model simulations. ALL represents
609 historical simulations with both anthropogenic and natural forcings,
610 RCP2.6/4.5/6.0/8.5 represent four representative concentration pathways from lower
611 to higher emission scenarios.

612 **Figure 4.** Spatial pattern of relative changes in multi-model ensemble mean
613 precipitation at 1.5, 2 and 3 °C warming levels compared to the baseline period
614 (1986-2005). The percentages in the upper-right corners of each panel are the
615 watershed-mean changes for different RCP scenarios, and the percentages in the top
616 brackets are the mean values from four RCP scenarios.

617 **Figure 5.** The same as **Figure 4**, but for the spatial patterns of runoff changes.

618 **Figure 6.** Comparison of the characteristics (amount (number of drought events per
619 20 years), duration (months) and severity) averaged among climate models and RCP
620 scenarios for hydrological drought events during the baseline period (1986-2005) and
621 the periods reaching 1.5, 2 and 3 °C warming levels. Black lines indicate 5%-95%

622 confidence intervals.

623 **Figure 7.** Comparison of (a) mean values and (b) standard deviations for hydrological
624 indices averaged among climate models and RCP scenarios during the baseline period
625 (1986-2005) and the periods reaching 1.5, 2 and 3 °C warming levels. SPI, SEI, SRI,
626 SSRI, SBI, SSI represent standardized indices of precipitation, evapotranspiration,
627 runoff, surface runoff, baseflow (subsurface runoff) and streamflow, respectively.

628 **Figure 8.** Fractions of uncertainties from internal variability (orange), RCP scenarios
629 (green) and climate and land surface hydrological models (blue) for the projections of
630 20-years moving averaged (a) temperature, (b) precipitation (c) streamflow and (d)
631 hydrological drought frequency. Two dashed lines indicate the multi-model ensemble
632 median years reaching 1.5 °C (year 2025), 2 °C (year 2042) and 3 °C (year 2070)
633 warming levels, respectively.

634

635 **Table Captions**

636 **Table 1.** CMIP5 model simulations used in this study. ALL represents historical
637 simulations with both anthropogenic and natural forcings (r1i1p1 realization),
638 RCP2.6/4.5/6.0/8.5 represent four representative concentration pathways from lower
639 to higher emission scenarios.

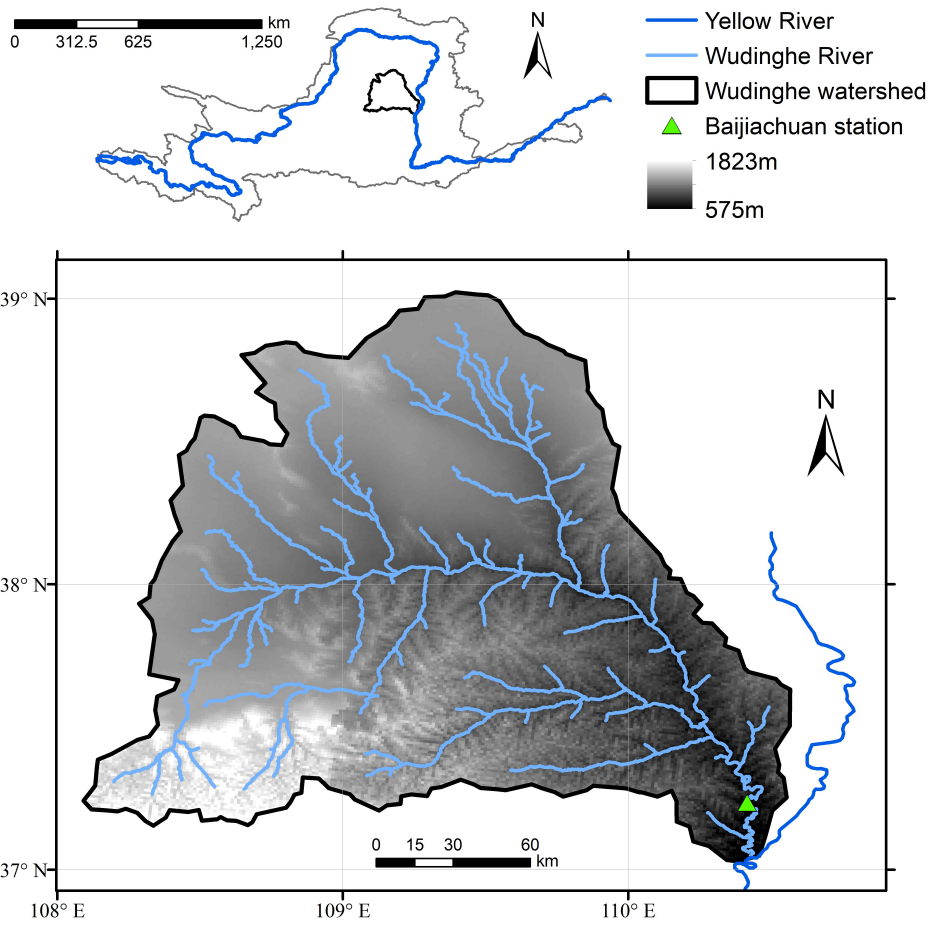
640 **Table 2.** Trends in hydrometeorological variables and hydrological drought frequency
641 over the Wudinghe watershed. Historical observed trends for streamflow and drought
642 frequency were calculated by using naturalized streamflow data (Yuan et al., 2017).

643 Here, “*” and “**” indicate 90% and 99% confidence levels, respectively, while those

644 without any “*” show no significant changes ($p>0.1$).

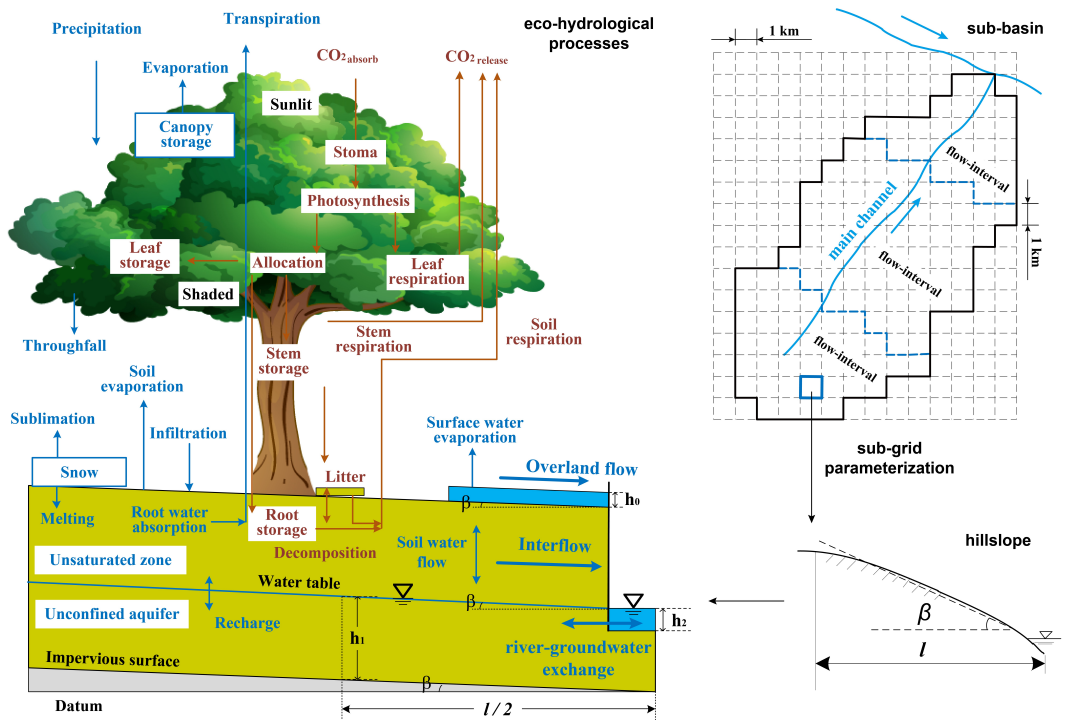
645 **Table 3.** Determination of crossing year for the periods reaching 1.5, 2 and 3 °C
646 warming levels for different GCMs and RCPs combinations. Here, “NR” means that
647 the corresponding GCM/RCP combination will not reach the specified warming level
648 throughout the 21st century.

649 **Table 4.** Uncertainty contributions (%) from internal variability, climate models and
650 RCPs scenarios for the future projections considering 1.5, 2 and 3 °C warming levels.



651

652 **Figure 1.** Location, elevation and river networks for the Wudinghe watershed.

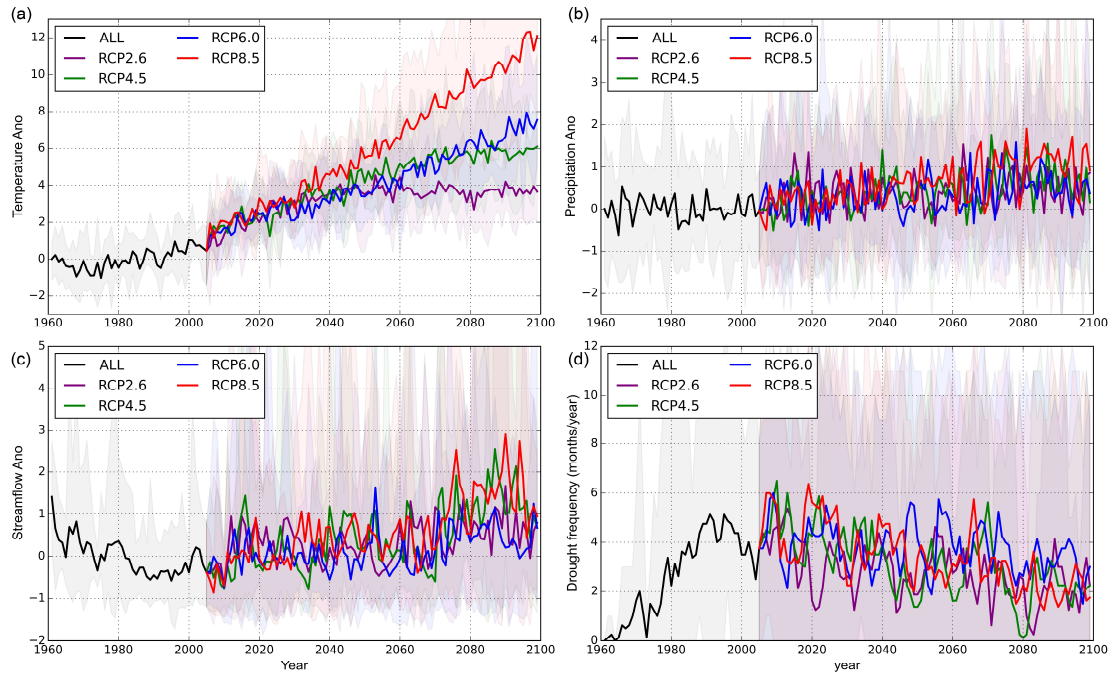


653

654 **Figure 2.** Structure and main eco-hydrological processes for the land surface

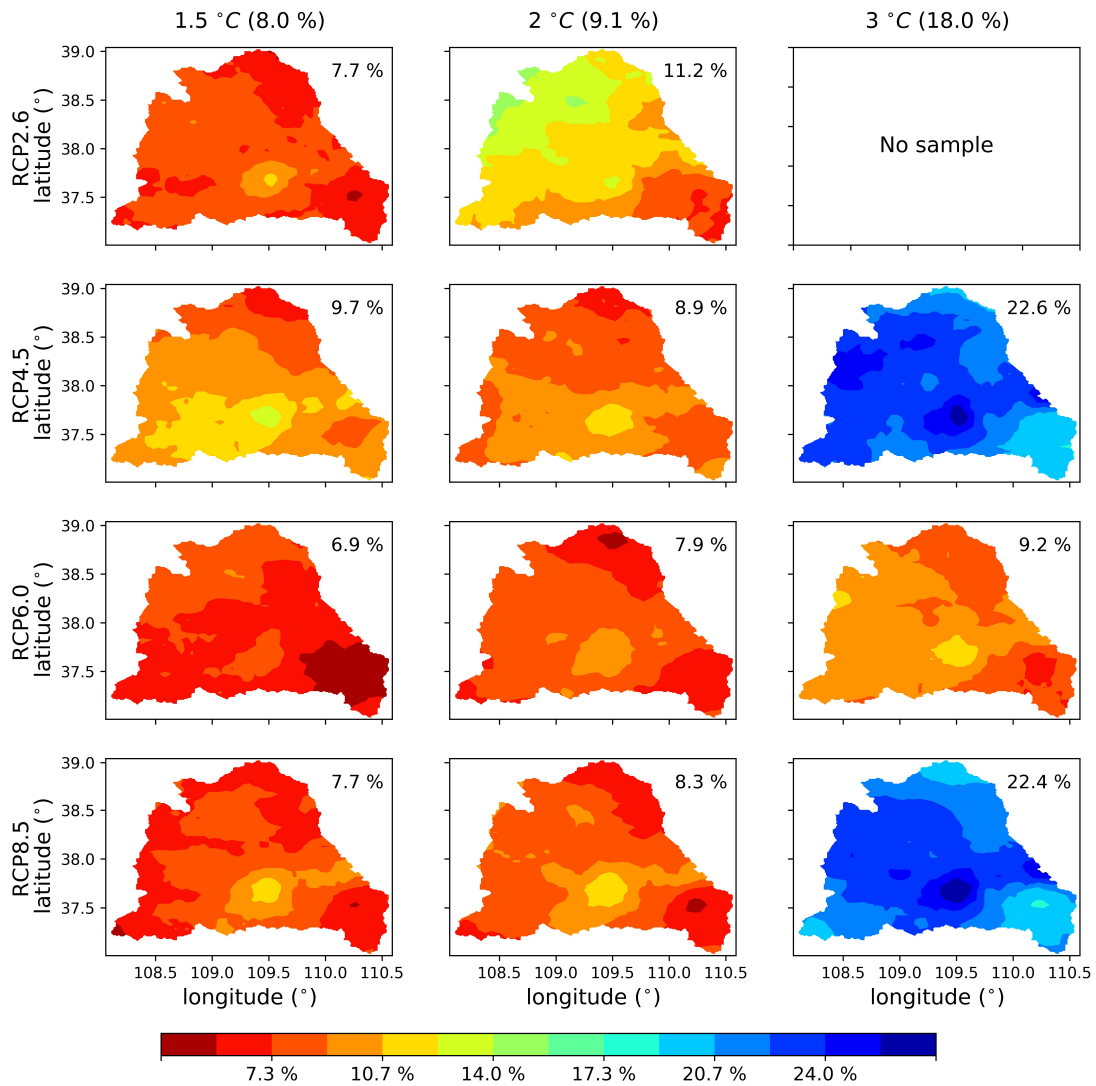
655 hydrological model CLM-GBHM. (modified from Jiao et al., 2017)

656



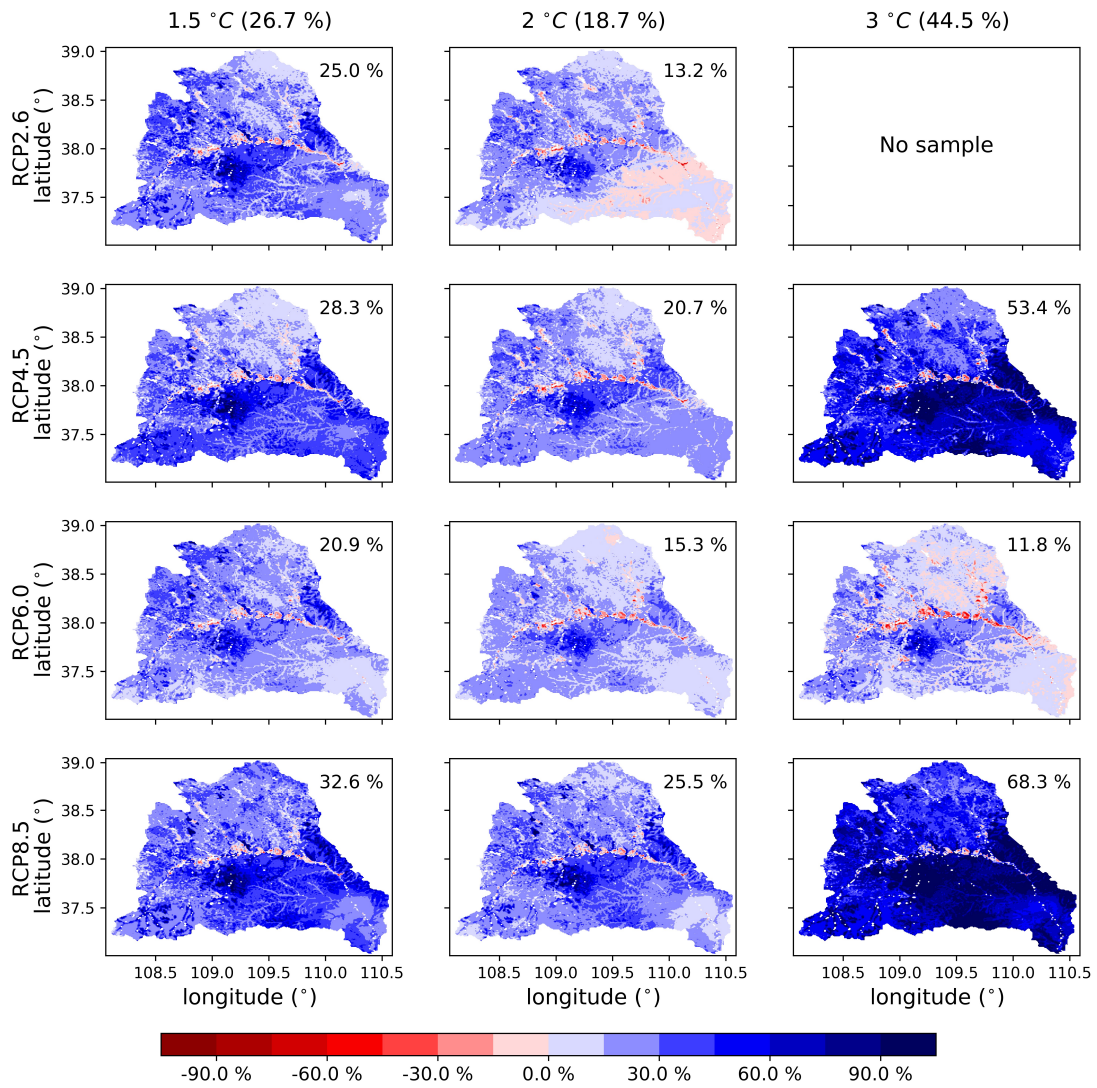
657

658 **Figure 3.** Historical (ALL) and future (RCP2.6/4.5/6.0/8.5) time series of
 659 standardized annual mean (a) temperature, (b) precipitation and (c) streamflow, and (d)
 660 the time series of hydrological drought frequency (drought months for each year) over
 661 the Wudinghe watershed. Shaded areas indicate the ranges between maximum and
 662 minimum values among CMIP5/CLM-GBHM model simulations. ALL represents
 663 historical simulations with both anthropogenic and natural forcings,
 664 RCP2.6/4.5/6.0/8.5 represent four representative concentration pathways from lower
 665 to higher emission scenarios.



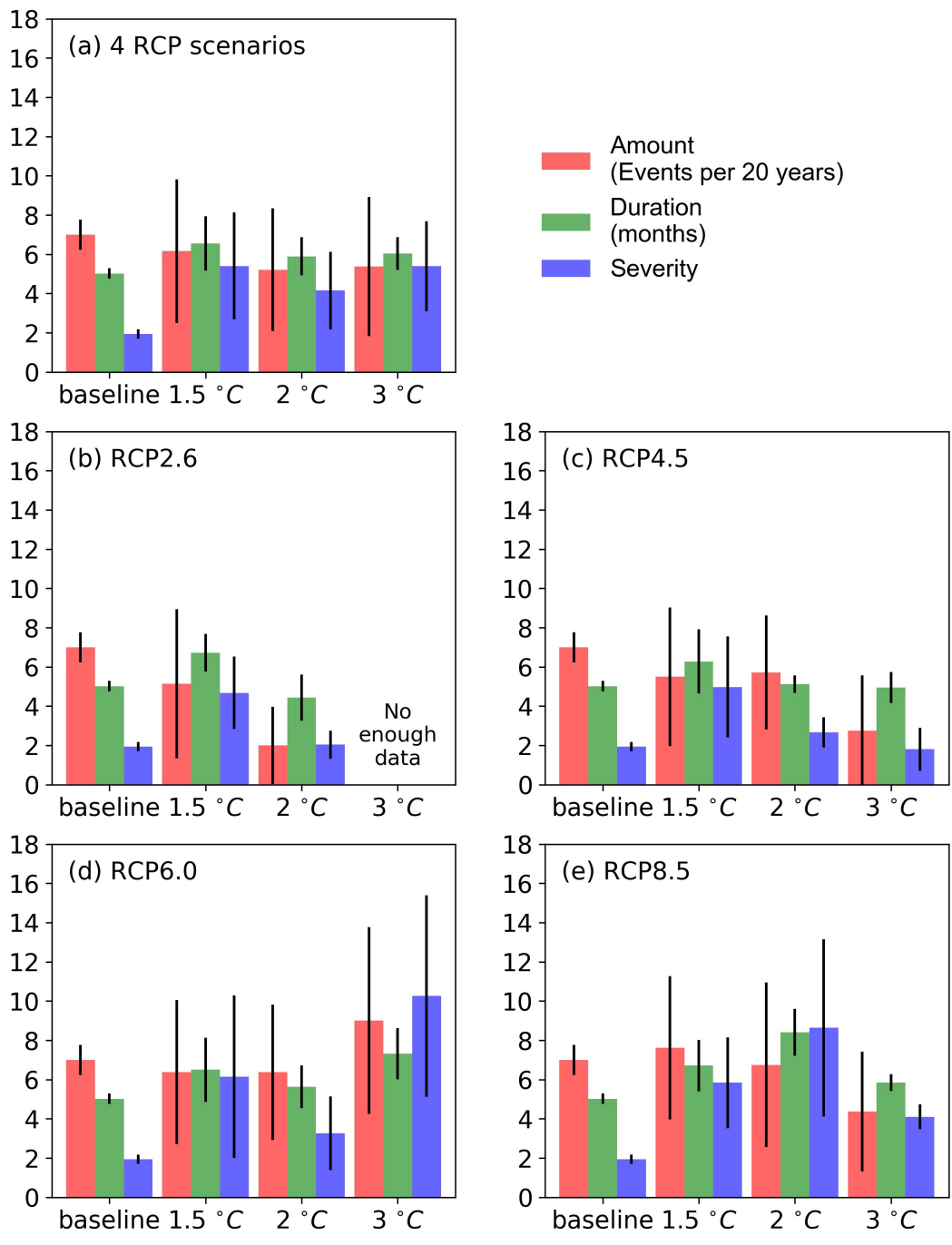
666

667 **Figure 4.** Spatial pattern of relative changes in multi-model ensemble mean
 668 precipitation at 1.5, 2 and 3 °C warming levels compared to the baseline period
 669 (1986-2005). The percentages in the upper-right corners of each panel are the
 670 watershed-mean changes for different RCP scenarios, and the percentages in the top
 671 brackets are the mean values from four RCP scenarios.



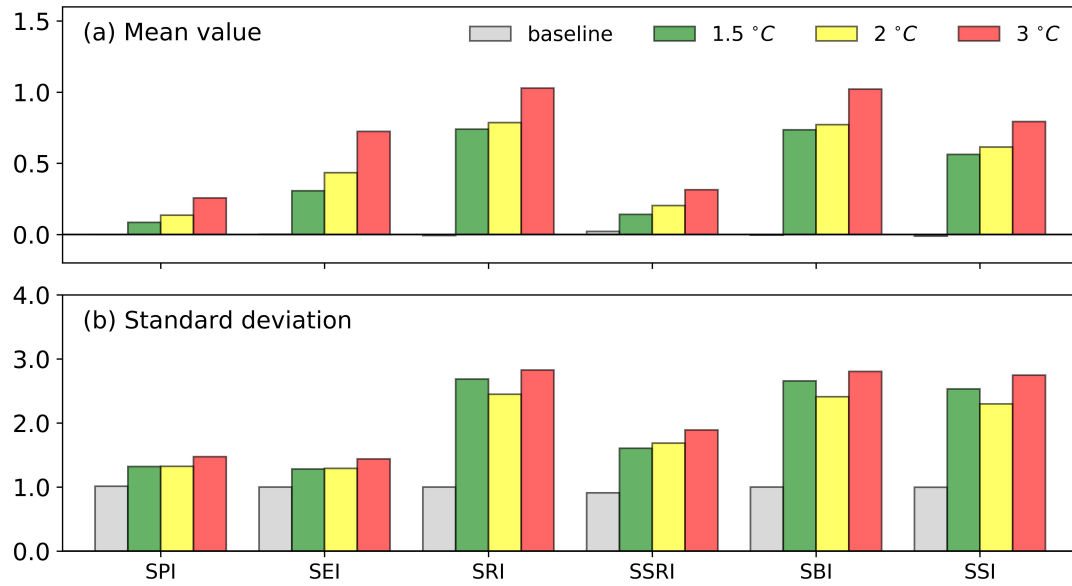
672

673 **Figure 5.** The same as **Figure 4**, but for the spatial patterns of runoff changes.



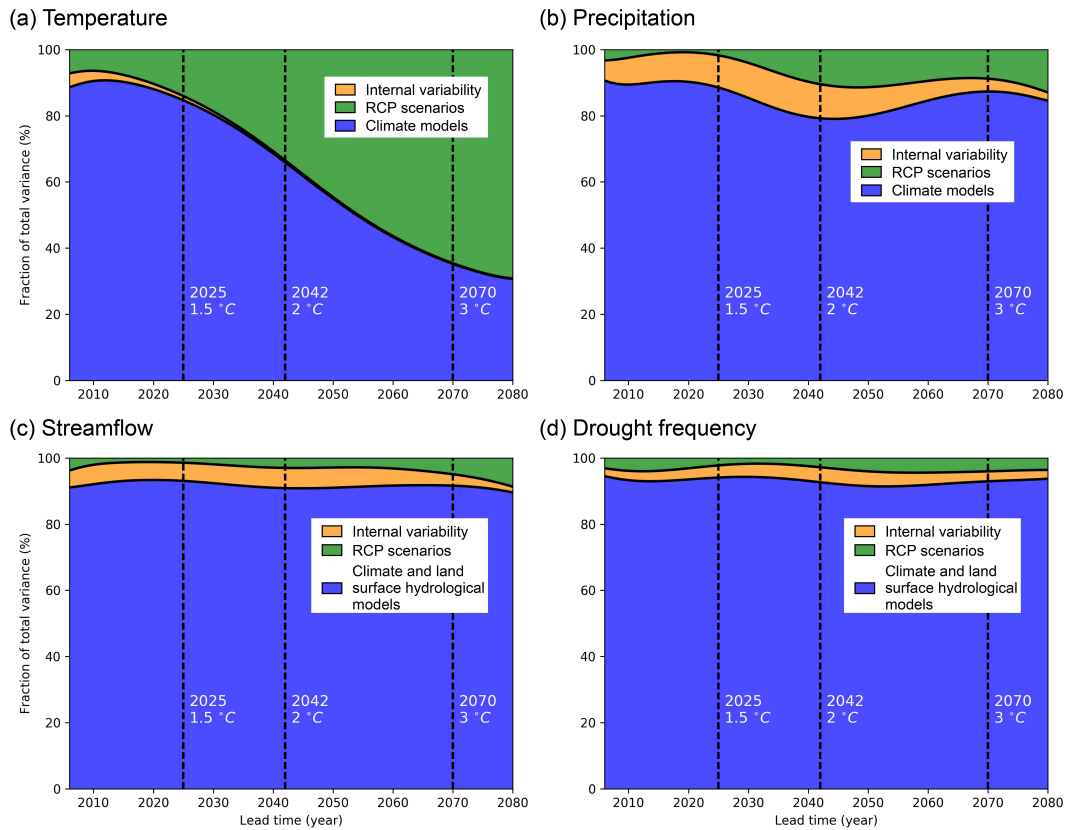
674

675 **Figure 6.** Comparison of the characteristics (amount (number of drought events per
 676 20 years), duration (months) and severity) averaged among climate models and RCP
 677 scenarios for hydrological drought events during the baseline period (1986-2005) and
 678 the periods reaching 1.5, 2 and 3 °C warming levels. Black lines indicate 5%-95%
 679 confidence intervals.



680

681 **Figure 7.** Comparison of (a) mean values and (b) standard deviations for hydrological
 682 indices averaged among climate models and RCP scenarios during the baseline period
 683 (1986-2005) and the periods reaching 1.5, 2 and 3 °C warming levels. SPI, SEI, SRI,
 684 SSRI, SBI, SSI represent standardized indices of precipitation, evapotranspiration,
 685 runoff, surface runoff, baseflow (subsurface runoff) and streamflow, respectively.



686

687 **Figure 8.** Fractions of uncertainties from internal variability (orange), RCP scenarios
 688 (green) and climate and land surface hydrological models (blue) for the projections of
 689 20-years moving averaged (a) temperature, (b) precipitation (c) streamflow and (d)
 690 hydrological drought frequency. Two dashed lines indicate the multi-model ensemble
 691 median years reaching 1.5 °C (year 2025), 2 °C (year 2042) and 3 °C (year 2070)
 692 warming levels, respectively.

693 **Table 1.** CMIP5 model simulations used in this study. ALL represents historical simulations with both anthropogenic and natural forcings
 694 (r1i1p1 realization), RCP2.6/4.5/6.0/8.5 represent four representative concentration pathways from lower to higher emission scenarios.

GCMs	Institute	Resolution	Historical simulations	RCP scenarios
GFDL-CM3	NOAA GFDL	144×90	ALL	RCP2.6/4.5/6.0/8.5
GFDL-ESM2M	NOAA GFDL	144×90	ALL	RCP2.6/4.5/6.0/8.5
HadGEM2-ES	MOHC	192×145	ALL	RCP2.6/4.5/6.0/8.5
IPSL-CM5A-LR	IPSL	96×96	ALL	RCP2.6/4.5/6.0/8.5
IPSL-CM5A-MR	IPSL	144×143	ALL	RCP2.6/4.5/6.0/8.5
MIROC-ESM-CHEM	MIROC	128×64	ALL	RCP2.6/4.5/6.0/8.5
MIROC-ESM	MIROC	128×64	ALL	RCP2.6/4.5/6.0/8.5
MRI-CGCM3	MRI	320×160	ALL	RCP2.6/4.5/6.0/8.5

695 **Table 2.** Trends in hydrometeorological variables and hydrological drought frequency over the Wudinghe watershed. Historical observed trends
696 for streamflow and drought frequency were calculated by using naturalized streamflow data (Yuan et al., 2017). Here, “*” and “**” indicate 90%
697 and 99% confidence levels, respectively, while those without any “*” show no significant changes ($p>0.1$).

Historical (1961-2005) and future (2006-2099) scenarios	Changing trend of standardized timeseries (yr ⁻¹)			
	Temperature	Precipitation	Streamflow	Drought frequency
(historical) observations	0.0494**	-0.0216*	-0.0503**	0.0448**
(historical) all forcings simulations	0.0272**	-0.0009	-0.0213**	0.0346**
(future) RCP2.6 simulations	0.0138**	0.0025*	0.0046**	-0.0069**
(future) RCP4.5 simulations	0.0291**	0.0056**	0.0105**	-0.0096**
(future) RCP6.0 simulations	0.0312**	0.0039**	0.0038**	-0.0044**
(future) RCP8.5 simulations	0.0345**	0.0108**	0.0133**	-0.0107**

698 **Table 3.** Determination of crossing year for the periods reaching 1.5, 2 and 3 °C warming levels for different GCMs and RCPs combinations.

699 Here, “NR” means that the corresponding GCM/RCP combination will not reach the specified warming level throughout the 21st century.

GCMs	1.5 °C warming level				2 °C warming level				3 °C warming level			
	RCP2.6	RCP4.5	RCP6.0	RCP8.5	RCP2.6	RCP4.5	RCP6.0	RCP8.5	RCP2.6	RCP4.5	RCP6.0	RCP8.5
GFDL-CM3	2016	2018	2019	2018	2039	2032	2039	2030	NR	2066	2070	2052
GFDL-ESM2M	NR	2051	2059	2038	NR	NR	2076	2054	NR	NR	NR	2084
HadGEM2-ES	2020	2023	2023	2018	2042	2039	2042	2032	NR	2071	2070	2052
IPSL-CM5A-LR	2030	2029	2031	2025	NR	2045	2049	2037	NR	NR	2086	2057
IPSL-CM5A-MR	2032	2025	2031	2024	NR	2045	2050	2037	NR	NR	2081	2055
MIROC-ESM-CHEM	2019	2024	2026	2020	2037	2038	2042	2032	NR	2075	2070	2051
MIROC-ESM	2026	2025	2032	2024	2048	2039	2046	2033	NR	2080	2076	2056
MRI-CGCM3	2075	2043	2053	2036	NR	2074	2070	2049	NR	NR	NR	2072
Model ensemble	2026	2025	2031	2024	2041	2039	2048	2035	NR	2073	2073	2056
Total ensemble	2025 (2016~2075)				2042 (2030~2076)				2070 (2051~2086)			

700

701 **Table 4.** Uncertainty contributions (%) from internal variability, climate models and RCPs scenarios for the future projections considering 1.5, 2
 702 and 3 °C warming levels.

Variables	1.5 °C warming level			2 °C warming level			3 °C warming level		
	Internal variability	Climate Models	RCPs scenarios	Internal variability	Climate Models	RCPs scenarios	Internal variability	Climate Models	RCPs scenarios
Temperature	1.4	84.4	14.3	0.7	66.3	33.0	0.2	36.1	63.7
Precipitation	9.7	87.8	2.5	10.1	80.4	9.5	4.1	86.3	9.6
Streamflow	5.6	92.8	1.6	6.0	91.2	2.8	3.5	91.3	5.1
Drought frequency	3.6	93.8	2.5	4.4	92.8	2.8	3.1	92.8	4.0

703